



Enhancing the $t\bar{t}H$ signal through top-quark spin polarization effects at the LHC

Sanjoy Biswas^{a,b}, Rikkert Frederix^c, Emidio Gabrielli^{d,e,f}, Barbara Mele^b

^a*Dipartimento di Fisica, Università di Roma “La Sapienza”, Piazzale Aldo Moro 2, I-00185 Rome, Italy*

^b*INFN, Sezione di Roma, Piazzale Aldo Moro 2, I-00185 Rome, Italy*

^c*PH Department, TH Unit, CERN, CH-1211 Geneva 23, Switzerland*

^d*Department of Physics, Theoretical Section, University of Trieste, Strada Costiera 11, I-34151 Trieste, Italy*

^e*INFN, Sezione di Trieste, Via Valerio 2, I-34127 Trieste, Italy*

^f*NICPB, Ravala 10, Tallinn 10143, Estonia*

Abstract

We consider the impact of the $t\bar{t}$ spin correlations in the Higgs boson production in association with top quark pairs $pp \rightarrow t\bar{t}H$ and in the corresponding backgrounds. We study the $H \rightarrow b\bar{b}$ and $H \rightarrow \gamma\gamma$ decay modes. We show that retaining the $t\bar{t}$ spin-correlation effects could significantly improve the LHC sensitivity to the $t\bar{t}H$ signal, particularly in the $H \rightarrow \gamma\gamma$ channel.

Keywords: top quark, Higgs boson, polarization, spin correlations, LHC

1. Introduction

The Higgs boson discovery in 2012 [1, 2] has been a great success of the Standard Model (SM) of electroweak (EW) interactions. All measurements are in quite good agreement with SM expectations for a Higgs boson mass of 125 GeV, leaving moderate room for potential new physics contributions. The forthcoming LHC run at 13 TeV is expected to consolidate both the indirect and the direct measurement of the Higgs boson couplings to fermions (Yukawa couplings). This represents a crucial test for the SM mechanism of chiral symmetry breaking and fermion mass generation.

In the SM framework, the Higgs Yukawa coupling to the top-quark (Y_t) is of particular phenomenological and theoretical interest. Being of order $O(1)$, Y_t is responsible for the vacuum stability of the Higgs potential and EW symmetry breaking [3]–[5], providing one of the leading contributions to the radiative corrections to the Higgs potential. On the other hand, the top Yukawa coupling enters the dominant Higgs production mechanism at the LHC through the effective gluon-gluon-Higgs (ggH) coupling [6] induced by top-quark loops. It is then crucial to have also direct information on Y_t ,

since this will allow to either confirm or disprove the SM mechanism for the origin of top-quark mass. The latter case would imply the existence of physics beyond the SM at the TeV scale. As a matter of fact, obtaining model-independent Y_t determinations is not straightforward at the LHC. Potential one-loop contributions from unknown new physics could in principle affect the effective ggH coupling in the main Higgs-boson production mechanism. This makes the top-quark Yukawa coupling determination through the $gg \rightarrow H$ production quite model dependent.

A less model-dependent test of Y_t at the LHC is provided by the study of the Higgs-boson production in association with a $t\bar{t}$ pair, $pp \rightarrow t\bar{t}H$ [7]–[17], where one can tag the actual presence of top quarks in the final state [18, 19]. The small corresponding cross section makes the $t\bar{t}H$ process a quite challenging channel. On the one hand, the phase-space depletes the heavy $t\bar{t}H$ final states, with a production cross section of just about 130 fb at 8 TeV [20]. On the other hand, disentangling the QCD background for the high-rate Higgs decay channel $H \rightarrow b\bar{b}$ makes the problem even harder. The QCD backgrounds mainly arise from the $t\bar{t}b\bar{b}$ and $t\bar{t}jj$ final states, whose corresponding fraction is about

few percents and more than 95% respectively [21]. The reconstruction of the $H \rightarrow b\bar{b}$ resonance is also plagued by a combinatorial background arising from the incorrect b -jet assignment due either to extra b 's from t and \bar{t} decays or misidentified light jets.

The challenge in the study of the high-statistics channel for $t\bar{t}H$ motivated dedicated analysis in the rarest Higgs decays, like $H \rightarrow \gamma\gamma$ and multi-leptons, where a more favorable signal-to-background ratio (S/B) can compensate for the lack of statistics. For instance, with the present data set at 7 TeV plus 8 TeV, a 95% C.L. observed upper limit of 5.2 (4.1) times the SM cross section has been set by CMS [22] (ATLAS [23]) in the $H \rightarrow b\bar{b}$ channel, where CMS result also include the $H \rightarrow \tau^+\tau^-$ channel. This should be compared with the 95% C.L. observed upper limit on the $H \rightarrow \gamma\gamma$ channels of 5.4 (5.3) times the SM cross section set by CMS [24] (ATLAS [25]). It is then crucial to develop new search strategies aimed to improve the separation of the signal from the $t\bar{t}H$ irreducible backgrounds.

The aim of the present study is to explore the potential of the spin-correlation properties in the associated Higgs top-pair production at the LHC as a possible strategy to enhance the sensitivity to the $t\bar{t}H$ signal.

It is well known that $t\bar{t}$ spin correlations can be a useful tool in different frameworks. For instance, they could help in disentangling the SM scalar component from a pseudoscalar non-standard one in the top-Higgs coupling [26]. In [27], it was emphasized that the relative impact of spin correlations on the leading-order (LO) $t\bar{t}H$ lepton kinematical distributions is much more dramatic than the impact of the corresponding QCD NLO corrections [16].

Here we focus on the two channels corresponding to the $H \rightarrow \gamma\gamma$ and $H \rightarrow b\bar{b}$ decays [28]

$$pp \rightarrow t\bar{t}H (\rightarrow \gamma\gamma) \quad (1)$$

$$pp \rightarrow t\bar{t}H (\rightarrow b\bar{b}), \quad (2)$$

where the corresponding irreducible backgrounds $t\bar{t}\gamma\gamma$ and $t\bar{t}b\bar{b}$ are expected to play a major role with respect to reducible ones.

Since the top-quark life time is shorter than the characteristic hadronization time scale, top quarks are expected to decay before their original spin is affected by strong interactions. This guarantees that the top-quark spin polarization at production level can be fully transferred to the top decay products. Hence, by reconstructing the individual top systems [29] the top-quark spin properties can be accessed by measuring suitable angular distributions of the final decay products in $t \rightarrow W + b \rightarrow \ell\nu(\text{du}) + b$ [30]. Among the top decay

products, the charged lepton (or d quark) angular distributions has the maximal spacial correlation with the original top-quark spin axis [31]-[32].

While the top quark and antiquark pairs are mostly unpolarized in the $t\bar{t}$ production at hadron colliders, their spins are strongly correlated. In particular, in the naïve chiral limit for the top mass ($m_t \rightarrow 0$), or for very large values of the $t\bar{t}$ invariant mass $m_{t\bar{t}} \gg m_t$, one expects that top-pairs are produced in the LR+RL helicity configuration, where L(R) stands for the left(right)-handed helicity polarization. On the other hand, the same naïve expectation suggests that the $t\bar{t}$ helicity configuration should also be correlated in the $t\bar{t}H$ production, but in a complementary way, with a dominant LL+RR configuration with respect to the LR+RL ones, the latter being suppressed by terms of order $O(m_t^2/m_{t\bar{t}}^2)$. This is because the Higgs boson emission from the top-quark line flips its chirality.

The actual helicity-configuration behaviour is shown in Fig. 1, where we report the results from [28] for the integrated top p_T distributions projected on the $t\bar{t}$ helicity configurations LL+RR and LR+RL (normalized to the total cross section), for the $t\bar{t}$ (left plot) and $t\bar{t}H$ (right plot) productions, in the Lab frame.

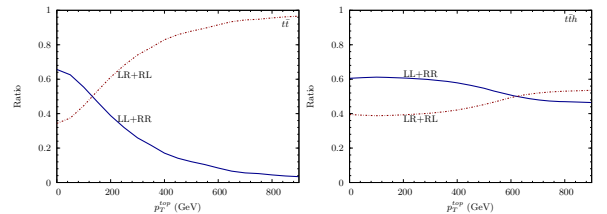


Figure 1: Integrated p_T^{top} distributions for the like-helicity top pairs ($t_L\bar{t}_L + t_R\bar{t}_R$) and unlike-helicity top pairs ($t_L\bar{t}_R + t_R\bar{t}_L$) in unpolarised $t\bar{t}$ (left plot) and $t\bar{t}H$ (right plot) samples, versus the hardest-top p_T^{top} cut at c.m. energy of 14 TeV, in the Lab frame.

Here, p_T^{top} is the minimum transverse momentum of the hardest top. As one can see, the helicity correlations are not quite complementary as expected in the top chiral limit. This is because the top-quark mass effects and the presence of an extra massive (Higgs) particle in the final state spoil the naïve expectations, at least for p_T^{top} lower than about 800 GeV. Then, the actual chiral limit is reached for much higher p_T^{top} values.

On the other hand, by applying similar naïve chirality arguments, one might conclude that the $t\bar{t}$ spins in the $t\bar{t}\gamma\gamma$ and $t\bar{t}b\bar{b}$ irreducible backgrounds should also be correlated, but in a complementary way with respect to the $t\bar{t}$ spins of the $t\bar{t}H$ signal. In fact the vector-like mediated interactions, induced by gluon and photon

emission from quarks (that are the interactions involved in the irreducible backgrounds) conserve chirality. We checked that this expectation is partially confirmed for the $t\bar{t}\gamma\gamma$ background, while it is not for the $t\bar{t}b\bar{b}$ one. Indeed, for the latter, the $t\bar{t}$ spin correlations turn out to be washed out in the integrated cross section, with a similar fraction of final LL+RR and LR+RL configurations. By applying basic cuts (that we will define later on), for the $H \rightarrow \gamma\gamma$ channel we find that about 61% of the total $t\bar{t}H$ cross section corresponds to the LL+RR combination, with a remaining 39% for LR+RL. As for the $t\bar{t}\gamma\gamma$ background, 28% (72%) of the total cross section corresponds to the LL+RR (LR+RL) combination.

Spin correlations in the hadronic $t\bar{t}$ production manifest in the angular distributions of top decay products in specific frames and coordinate basis, where they can be directly measured [33]–[35]. In this work we focus on the $\frac{d\sigma}{d\cos\varphi}$ distributions, where φ stands for the angle between the three-momenta of one of the top decay products and one of the anti-top decay products. These distributions are frame dependent. We will consider, apart from the usual laboratory frame, two further reference frames where the $t\bar{t}$ spin correlations effects are known to be particularly enhanced [34]. In particular, we consider the angular distributions corresponding to the angle φ between the direction of flight of ℓ^+ (b) in the t rest system and ℓ^- (\bar{b}) in the \bar{t} rest system [34]. In order to avoid ambiguities, one has to specify the common initial frame where the Lorentz boosts are applied in order to separately bring the t and \bar{t} at rest. We call *Frame-1* and *Frame-2* the two frames where the t and \bar{t} rest systems are obtained, respectively, by two rotation-free Lorentz boosts [28], [33]–[35]

- with respect to the $t\bar{t}$ -pair c.m. frame (Frame-1),
- with respect to the laboratory frame (Frame-2).

We consider the following variables, that are particularly sensitive to spin correlations, namely $\cos\theta_{\ell\ell}$, where $\theta_{\ell\ell}$ is the three-dimensional polar angle between the ℓ^+ and ℓ^- directions of flight, and analogously, the $\cos\theta_{b\bar{b}}$ variable that involves the two b quarks from t and \bar{t} decays.

In the following we will show a few particularly significant plots for the signal (background) angular distributions, detailed through red (green) lines, while spin-correlated (-uncorrelated) cases will be reported through solid (dashed) lines. A more complete study, can be found in [28]. For both signal and background the $t \rightarrow b\ell\nu$ decay has been performed in MadGraph5 [36] by retaining the full spin information, while, in the uncorrelated case, the spin polarization effects have been

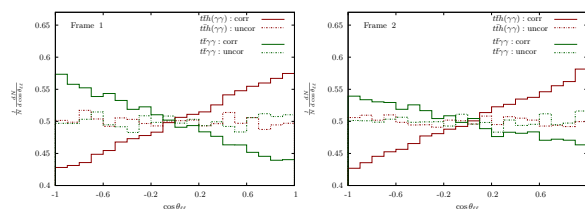


Figure 2: The $\cos\theta_{\ell\ell}$ distribution for the signal $t\bar{t}H(H \rightarrow \gamma\gamma)$ (red) and $t\bar{t}\gamma\gamma$ background (green), with (solid) and without (dashed) spin information, in Frame-1 (left) and Frame-2 (right). The cuts $p_T^{\gamma_{1,2}} > 20$ GeV, $|\eta_{\gamma_{1,2}}| < 2.5$ and $\Delta R_{\gamma_1\gamma_2} > 0.4$ have been imposed on photons, in addition to the invariant mass cut $123 \text{ GeV} < m_{\gamma\gamma} < 129 \text{ GeV}$.

neglected in the decay by interfacing MadGraph5 with PYTHIA [37] before the $t\bar{t}$ decays. Our analysis does not include shower nor hadronization effects. All distributions that will be presented are normalized to 1.

2. Top spin correlations in the $t\bar{t}\gamma\gamma$ channel

We consider now the signal and irreducible background for the $t\bar{t}\gamma\gamma$ channel in both correlated and uncorrelated analysis. In this case, we impose the following kinematical cuts on the photons' transverse momenta, $p_T^{\gamma_{1,2}} > 20$ GeV, pseudorapidities, $|\eta_{\gamma_{1,2}}| < 2.5$, and isolation, $\Delta R_{\gamma_1\gamma_2} > 0.4$, in addition to a diphoton invariant mass cut $123 \text{ GeV} < m_{\gamma\gamma} < 129 \text{ GeV}$, where ΔR_{ij} is as usual $\Delta R_{ij} = \sqrt{\eta_{ij}^2 + \phi_{ij}^2}$, with $\eta_{ij}(\phi_{ij})$ the rapidity (azimuthal) separation.

Final results for the $\cos\theta_{\ell\ell}$ distribution for the signal $t\bar{t}H(H \rightarrow \gamma\gamma)$ and $t\bar{t}\gamma\gamma$ background are shown in Fig.2. One can see that, neglecting spin correlations, the angular distributions for the signal and background are both flat in $\cos\theta_{\ell\ell}$, in both reference frames. On the contrary, when the spin information is taken into account, the signal and background distributions are different and quite complementary. In particular, the signal (background) distribution is monotonically increasing (decreasing) as a function of $\cos\theta_{\ell\ell}$. This is a consequence of the aforementioned complementarity in the $t\bar{t}$ helicity correlations of the signal and irreducible background for the $H \rightarrow \gamma\gamma$ channel, previously discussed. Although the correlation effect is remarkable both in Frame-1 and Frame-2, the separation between the correlated $\cos\theta_{\ell\ell}$ distributions for signal and background is maximized in Frame-1, where one gets an improvement in S/B (computed by integrating angular distributions over the range $0 < \cos\theta_{\ell\ell} < 1$) of about 17%, compared to the uncorrelated case. The corresponding distributions in the $\cos\theta_{b\bar{b}}$ variable in Frame-1 are all approximately flat,

and no significant effect is found in this case. Analogous results hold in Frame-2.

We also considered for comparison various distributions in the laboratory frame (Lab Frame), where the variables studied are more straightforward to reconstruct experimentally. Although in the Lab Frame the inclusion of spin correlations increases the difference in distribution shapes between signal and background, the relative effect is quite smaller than in Frame 1 and Frame 2 for leptonic distributions. This is shown in Fig. 3, where we present the correlated and uncorrelated distributions in $\cos\theta_{\ell\ell}$ and $\Delta\eta_\ell$ (top), and $\cos\theta_{b\bar{b}}$ and $\Delta\eta_b$ (bottom) (where $\Delta\eta_\ell \equiv |\eta_{\ell^+} - \eta_{\ell^-}|$, and $\Delta\eta_b \equiv |\eta_b - \eta_{\bar{b}}|$).

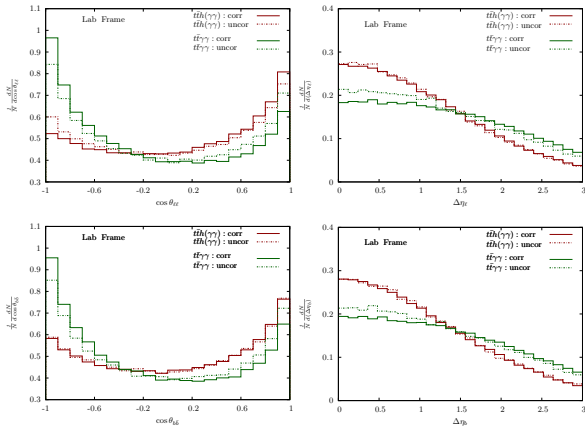


Figure 3: The $\cos\theta_{\ell\ell}$ (top left), $\Delta\eta_\ell$ (top right), $\cos\theta_{b\bar{b}}$ (bottom left), and $\Delta\eta_b$ (bottom right) distributions for the signal $t\bar{t}H(H \rightarrow \gamma\gamma)$ (red) and $t\bar{t}\gamma\gamma$ background (green), with (solid) and without (dashed) spin information, in the Lab frame. Same cuts as in Fig.2 have been imposed.

In Fig.4, we show the effects induced when including the contributions of photon emission from the t and \bar{t} charged decay products in the irreducible $\gamma\gamma$ continuum, in Frame-1 and Frame-2. To this end, additional kinematic cuts are required for photon and b -jet isolation, namely for transverse momenta $p_T^{b,\gamma_{1,2}} > 20$ GeV, $p_T^\ell > 10$ GeV, rapidities $|\eta^b| < 4.7$, $|\eta^\ell| < 2.7$, $|\eta^\gamma| < 2.5$, angular separations $\Delta R(bb, \ell\ell, \gamma\gamma, b\ell, b\gamma, \ell\gamma) > 0.4$, and invariant mass $m_{\gamma\gamma}$ of the diphoton system 123 GeV $< m_{\gamma\gamma} < 129$ GeV. From Fig.4, we can see that the $\cos\theta_{\ell\ell}$ distributions for the signal are basically unaffected by the new selection cuts. On the other hand, in the background the extra photon radiation tends to reduce the gap between the correlated and uncorrelated $\cos\theta_{\ell\ell}$ distributions. In particular, for Frame-1, one gets now an improvement by 14% in S/B .

Analogous results, but for the Lab Frame, are reported in Fig.5, where we show the $\cos\theta_{\ell\ell}$ (top left), $\Delta\eta_\ell$

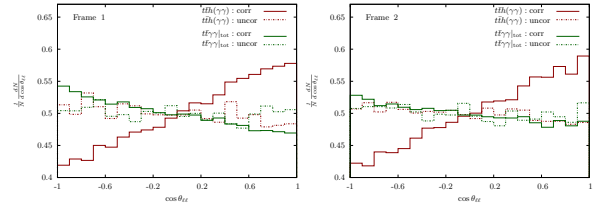


Figure 4: The $\cos\theta_{\ell\ell}$ distribution for the signal $t\bar{t}H(H \rightarrow \gamma\gamma)$ (red) and full $\gamma\gamma$ background (green) [including radiation from t, \bar{t} decay products, as defined in the text], with (solid) and without (dashed) spin information, in Frame-1 (left) and Frame-2 (right). Cuts described in the text have been applied to both signal and background.

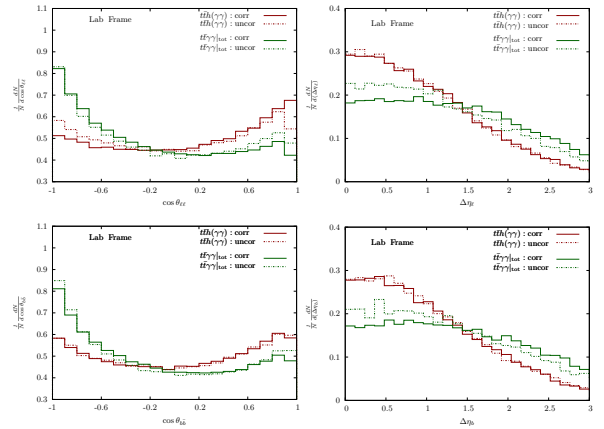


Figure 5: The $\cos\theta_{\ell\ell}$ (top left), $\Delta\eta_\ell$ (top right), $\cos\theta_{b\bar{b}}$ (bottom left), and $\Delta\eta_b$ (bottom right) distributions for the signal $t\bar{t}H(H \rightarrow \gamma\gamma)$ (red) and full $\gamma\gamma$ background (green) [including radiation from $t\bar{t}$ decay products, as defined in the text], with (solid) and without (dashed) spin information, in the Lab frame. Same cuts as in Fig.4 have been imposed.

(top right), $\cos\theta_{b\bar{b}}$ (bottom left) and $\Delta\eta_b$ (bottom right) distributions, including extra photon radiation from the decay products of top quarks, and the selection cuts just described above. One can see that for the Lab frame, the effects of photon emission from the top decay products do not dramatically affect the results where these contributions are ignored (cf. Fig. 3). Differences mainly show up for low separations of lepton and b pairs (that is for $\cos\theta_{\ell\ell}$, $\cos\theta_{b\bar{b}} \sim 1$ and $\Delta\eta_\ell, \Delta\eta_b < 1$), where the new set of cuts is more effective.

We have also studied spin correlations in the channel $t\bar{t}H(H \rightarrow b\bar{b})$, assuming to be able to distinguish the b quarks coming from top (anti top) decays from the b quarks coming from other sources (notably, from either Higgs decay or gluon radiation). Although spin-correlations affect considerably both signal and background distributions also in this case, they tend to differentiate the signal and the background less than in the $t\bar{t}H(H \rightarrow \gamma\gamma)$ channel. A detailed discussion on the

$t\bar{t}H(H \rightarrow b\bar{b})$ case can be found in [28].

3. Conclusions

We have investigated the advantages of taking into account $t\bar{t}$ spin-correlation effects in the measurement of the $t\bar{t}H$ process versus its irreducible backgrounds. We have considered the $t\bar{t}H(H \rightarrow \gamma\gamma)$ and $t\bar{t}H(H \rightarrow b\bar{b})$ channels, where irreducible backgrounds are expected to become more and more relevant in the LHC studies at 13 TeV. We showed that for the $t\bar{t}H(H \rightarrow \gamma\gamma)$ channel there is a significant advantage in employing a full $t\bar{t}$ spin-correlated analysis, which enhances the signal sensitivity with respect to the irreducible background. We found that there are indeed angular variables defined in dedicated reference frames, which could sizably increase the separation of signal and background, with a gain of up to 30% in S/B , in particular phase-space regions.

The present study suffers from a series of limitations that have to be overcome in order to quantify the actual potential of the proposed optimization strategy. We have not included reducible backgrounds, although irreducible backgrounds will get more and more important in future LHC analyzes. Next-to-Leading Order (NLO) QCD corrections, as well as parton-shower effects, should be included. Furthermore, we have assumed a 100% top-system reconstruction efficiency, although we are considering the challenging dilepton final state containing two neutrinos. Detection and resolution experimental effects can partly wash out our results in a more realistic environment, as discussed in [38] for the $t\bar{t}$ production. In the $t\bar{t}h$ case, the lower top-pair production statistics will make the top reconstruction even harder. On the other hand, the top reconstruction issues should mildly affect the spin-correlation results in the Lab frame, which anyhow is not the optimal frame to implement the present strategy.

In conclusion, we have found that spin-correlation features in the $t\bar{t}H$ production are a quite promising tool for enhancing the signal sensitivity over the irreducible background. They should then be taken into account in a more systematic way in future analyzes of the $t\bar{t}H$ process at the LHC at higher integrated luminosities.

References

- [1] G. Aad *et al.* [ATLAS Collaboration], “Observation of a new particle in the search for the Standard Model Higgs boson with the ATLAS detector at the LHC,” *Phys. Lett. B* **716** (2012) 1 [arXiv:1207.7214 [hep-ex]].
- [2] S. Chatrchyan *et al.* [CMS Collaboration], “Observation of a new boson at a mass of 125 GeV with the CMS experiment at the LHC,” *Phys. Lett. B* **716** (2012) 30 [arXiv:1207.7235 [hep-ex]].
- [3] G. Degrandi, S. Di Vita, J. Elias-Miro, J. R. Espinosa, G. F. Giudice, G. Isidori and A. Strumia, *JHEP* **1208**, 098 (2012) [arXiv:1205.6497 [hep-ph]].
- [4] G. Isidori, G. Ridolfi and A. Strumia, *Nucl. Phys. B* **609**, 387 (2001) [hep-ph/0104016].
- [5] C. Ford, I. Jack and D. R. T. Jones, *Nucl. Phys. B* **387**, 373 (1992) [Erratum-ibid. *B* **504**, 551 (1997)] [hep-ph/0111190].
- [6] H. M. Georgi, S. L. Glashow, M. E. Machacek and D. V. Nanopoulos, *Phys. Rev. Lett.* **40**, 692 (1978).
- [7] Z. Kunszt, “Associated Production of Heavy Higgs Boson with Top Quarks,” *Nucl. Phys. B* **247** (1984) 339.
- [8] W. J. Marciano and F. E. Paige, “Associated production of Higgs bosons with $t\bar{t}$ pairs,” *Phys. Rev. Lett.* **66** (1991) 2433.
- [9] J. F. Gunion, “Associated top anti-top Higgs production as a large source of WH events: Implications for Higgs detection in the lepton neutrino gamma gamma final state,” *Phys. Lett. B* **261** (1991) 510.
- [10] W. Beenakker, S. Dittmaier, M. Kramer, B. Plumper, M. Spira and P. M. Zerwas, “Higgs radiation off top quarks at the Tevatron and the LHC,” *Phys. Rev. Lett.* **87** (2001) 201805 [hep-ph/0107081].
- [11] W. Beenakker, S. Dittmaier, M. Kramer, B. Plumper, M. Spira and P. M. Zerwas, “NLO QCD corrections to $t\bar{t}H$ production in hadron collisions,” *Nucl. Phys. B* **653** (2003) 151 [hep-ph/0211352].
- [12] L. Reina and S. Dawson, “Next-to-leading order results for $t\bar{t}H$ production at the Tevatron,” *Phys. Rev. Lett.* **87** (2001) 201804 [hep-ph/0107101].
- [13] S. Dawson, L. H. Orr, L. Reina and D. Wackerroth, “Associated top quark Higgs boson production at the LHC,” *Phys. Rev. D* **67** (2003) 071503 [hep-ph/0211438].
- [14] S. Dawson, C. Jackson, L. H. Orr, L. Reina and D. Wackerroth, “Associated Higgs production with top quarks at the large hadron collider: NLO QCD corrections,” *Phys. Rev. D* **68** (2003) 034022 [hep-ph/0305087].
- [15] S. Dittmaier, M. Kramer, I and M. Spira, “Higgs radiation off bottom quarks at the Tevatron and the CERN LHC,” *Phys. Rev. D* **70** (2004) 074010 [hep-ph/0309204].
- [16] R. Frederix, S. Frixione, V. Hirschi, F. Maltoni, R. Pittau and P. Torrielli, “Scalar and pseudoscalar Higgs production in association with a top-antitop pair,” *Phys. Lett. B* **701** (2011) 427 [arXiv:1104.5613 [hep-ph]].
- [17] M. V. Garzelli, A. Kardos, C. G. Papadopoulos and Z. Trócsányi, “Standard Model Higgs boson production in association with a top anti-top pair at NLO with parton showering,” *Europhys. Lett.* **96** (2011) 11001 [arXiv:1108.0387 [hep-ph]].
- [18] F. Maltoni, D. L. Rainwater and S. Willenbrock, “Measuring the top quark Yukawa coupling at hadron colliders via $t\bar{t}H, H \rightarrow W^+W^-$,” *Phys. Rev. D* **66** (2002) 034022 [hep-ph/0202205].
- [19] A. Belyaev and L. Reina, “ $pp \rightarrow t\bar{t}H, H \rightarrow \tau\tau$: Toward a model independent determination of the Higgs boson couplings at the LHC,” *JHEP* **0208** (2002) 041 [hep-ph/0205270].
- [20] S. Dittmaier *et al.* [LHC Higgs Cross Section Working Group Collaboration], “Handbook of LHC Higgs Cross Sections: 1. Inclusive Observables,” arXiv:1101.0593 [hep-ph].
- [21] S. Heinemeyer *et al.* [LHC Higgs Cross Section Working Group Collaboration], “Handbook of LHC Higgs Cross Sections: 3. Higgs Properties,” arXiv:1307.1347 [hep-ph].
- [22] CMS Collaboration, “Search for Higgs Boson Production in Association with a Top-Quark Pair and Decaying to Bottom Quarks or Tau Leptons,” CMS-PAS-HIG-13-019.

- [23] The ATLAS collaboration, ATLAS-CONF-2014-011, ATLAS-COM-CONF-2014-004.
- [24] CMS Collaboration, “Search for $t\bar{t}H$ production in events where H decays to photons at 8 TeV collisions,” CMS-PAS-HIG-13-015.
- [25] The ATLAS collaboration, “Search for $t\bar{t}H$ production in the $H \rightarrow \gamma\gamma$ channel at $\sqrt{s} = 8$ TeV with the ATLAS detector,” ATLAS-CONF-2013-080.
- [26] J. Ellis, D. S. Hwang, K. Sakurai and M. Takeuchi, “Disentangling Higgs-Top Couplings in Associated Production,” arXiv:1312.5736 [hep-ph].
- [27] P. Artoisenet, R. Frederix, O. Mattelaer and R. Rietkerk, “Automatic spin-entangled decays of heavy resonances in Monte Carlo simulations,” JHEP **1303** (2013) 015 [arXiv:1212.3460 [hep-ph]].
- [28] S. Biswas, R. Frederix, E. Gabrielli and B. Mele, JHEP **1407**, 020 (2014) [arXiv:1403.1790 [hep-ph]].
- [29] G. Aad et al. [ATLAS Collaboration], “Observation of spin correlation in $t\bar{t}$ events from pp collisions at $\sqrt{s} = 7$ TeV using the ATLAS detector,” Phys. Rev. Lett. **108** (2012) 212001 [arXiv:1203.4081 [hep-ex]]; ATLAS Collaboration, “Measurement of spin correlations in top-antitop events from proton-proton collisions at $\sqrt{s} = 7$ TeV using the ATLAS detector,” ATLAS-CONF-2013-101.
- [30] M. Beneke, I. Eftymiopoulos, M. L. Mangano, J. Womersley, A. Ahmadov, G. Azuelos, U. Baur and A. Belyaev et al., “Top quark physics,” In *Geneva 1999, Standard model physics (and more) at the LHC* 419-529 [hep-ph/0003033]; F. -P. Schilling, “Top Quark Physics at the LHC: A Review of the First Two Years,” Int. J. Mod. Phys. A **27** (2012) 1230016 [arXiv:1206.4484 [hep-ex]].
- [31] M. Jezabek, “Top quark physics,” Nucl. Phys. Proc. Suppl. **37B** (1994) 197 [hep-ph/9406411].
- [32] A. Brandenburg, Z. G. Si and P. Uwer, “QCD corrected spin analyzing power of jets in decays of polarized top quarks,” Phys. Lett. B **539** (2002) 235 [hep-ph/0205023].
- [33] W. Bernreuther, A. Brandenburg, Z. G. Si and P. Uwer, “Top quark spin correlations at hadron colliders: Predictions at next-to-leading order QCD,” Phys. Rev. Lett. **87** (2001) 242002 [hep-ph/0107086].
- [34] W. Bernreuther, A. Brandenburg, Z. G. Si and P. Uwer, “Top quark pair production and decay at hadron colliders,” Nucl. Phys. B **690** (2004) 81 [hep-ph/0403035].
- [35] W. Bernreuther and Z. -G. Si, “Distributions and correlations for top quark pair production and decay at the Tevatron and LHC.,” Nucl. Phys. B **837** (2010) 90 [arXiv:1003.3926 [hep-ph]].
- [36] J. Alwall, M. Herquet, F. Maltoni, O. Mattelaer and T. Stelzer, “MadGraph5 : Going Beyond,” JHEP **1106** (2011) 128 [arXiv:1106.0522 [hep-ph]].
- [37] T. Sjostrand, S. Mrenna and P. Z. Skands, “PYTHIA 6.4 Physics and Manual,” JHEP **0605** (2006) 026 [hep-ph/0603175].
- [38] M. Baumgart and B. Tweedie, “A New Twist on Top Quark Spin Correlations,” JHEP **1303** (2013) 117 [arXiv:1212.4888 [hep-ph]].